ADVANCED MATERIALS
www.advmat.de

Direct Chiral Discrimination with NMR

*Sagar Wadhwa, Dominique Buyens, and Jan G. Korvink**

Unaided nuclear magnetic resonance (NMR) spectroscopy is considered incapable of distinguishing enantiomers. However, as first derived by A.D. Buckingham, the tensor coupling the electric and magnetic dipoles is space-dependent, which varies according to the molecular structure, hence, would be different for two enantiomers. Exploiting the odd-parity coupling tensor, a new variant of a double-resonant radiofrequency (RF) NMR detector is developed, which is sensitive to both electric and magnetic dipoles. Using the detector, a new method for liquid-state NMR is developed and elaborated, with which two enantiomers are successfully discriminated.

1. Introduction

The chirality of a molecule is a fundamental property of its structure that can have a crucial impact on its function in biochemical and chemical reactions. In the pharmaceutical industry, it is estimated that half of the drugs currently synthesized are chiral in nature,[1,2] in which the therapeutic effects associated with one enantiomeric form are not necessarily reproduced by its mirror image. Therefore, it is important in drug discovery to distinguish the enantiomer with the desired biological activity from its inactive, or in some cases, toxic counterpart, such as in the case of thalidomide.[3–5] Nuclear magnetic resonance (NMR) can elucidate chemical structure down to atomic resolution. It is therefore remarkable that NMR in its standard mode of application is completely blind w.r.t. molecular chirality. This purely structural aspect implies that two enantiomers neither differ in atomic constituents nor bond connectivity. The NMR process is, in itself, achiral, since the nuclear shielding tensor responsible for chemical shifts due to the Zeeman effect is even under parity. Since enantiomeric differentiation has important consequences in chemistry and biology, the ability to distinguish enantiomers should be part of the standard toolkit of structure elucidation by NMR spectroscopy. Due to the importance of chirality, numerous workarounds have been devised that indirectly allow for enantiomeric discrimination via NMR spectroscopy.[6–14] This is achieved by altering the chemical environment of a molecule through the addition of chiral derivatizing agents or chiral solvating agents. However, such techniques suffer from complex derivatization, peak overlap between the chiral agent, and compounds of interest, as well as additional purification steps in order to recover costly compounds. In 2004, the first attempt at direct chiral discrimination was put forward by A.D. Buckingham,[15] to derive the conditions whereby the coupling between the electric and magnetic dipole could be directly circumvented. Following this, several attempts have been made at implementing this concept experimentally,[16–18] yet the direct and quantitative discrimination via NMR has remained elusive.

It was shown by Buckingham[16] that a chiral molecule, when placed in a static magnetic field, induces an electric nuclear shielding tensor, analogous to the NMR nuclear shielding tensor, which has the opposite sense of two enantiomers, and vanishes for achiral molecules. This chirality tensor, appearing in an extended NMR Hamiltonian, depends on the coupling between the rotating magnetic moment with the electric dipole for an atom.[16] The strength of the chirality tensor depends on various factors, such as the electronegativity of the atom, the molecular arrangement, gyromagnetic ratio, etc.[19] Thus potentially, at least two ways exist to distinguish chiral molecules by NMR, either to detect the growing oscillating electric dipole in response to a $\pi/2$ radiofrequency (RF) magnetic field $B_1(t)$ pulse being applied to the sample, or reciprocally, to detect the emerging oscillating magnetic moment when an RF electric field pulse $E_2(t)$ is applied to the sample to accumulate the enantiomerically induced phase.[16]

The first reported attempt to produce a functioning chiral detector was based on a ring-loop resonator design.[18] The design was based on the concept that, by reducing the magnetic field associated with an oscillating electric field, for example by adapting the geometry of the resonator with two counter loops, one can effectively suppress the Zeeman term of the Hamiltonian, which in this case would be noise. This created a sensitive volume in the resonator which was suitable for the NMR chiral measurements. A sample placed away from this volume would not have generated a signal from the chirality tensor. Nevertheless, it was acknowledged by the authors that the resonator could be used as an exciter, but not as a suitable detector. A solution could have

S. Wadhwa
Voxalytic GmbH
Rosengarten 3, 76228 Karlsruhe, Germany
S. Wadhwa, D. Buyens, J. G. Korvink
Institute of Microstructure Technology
Karlsruhe Institute of Technology
Hermann-von-Helmholtz-Platz 1, 76334 Eggenstein-Leopoldshafen, Germany
E-mail: jan.korvink@kit.edu

The ORCID identification number(s) for the author(s) of this article can be found under https://doi.org/10.1002/adma.202408547

DOI: 10.1002/adma.202408547

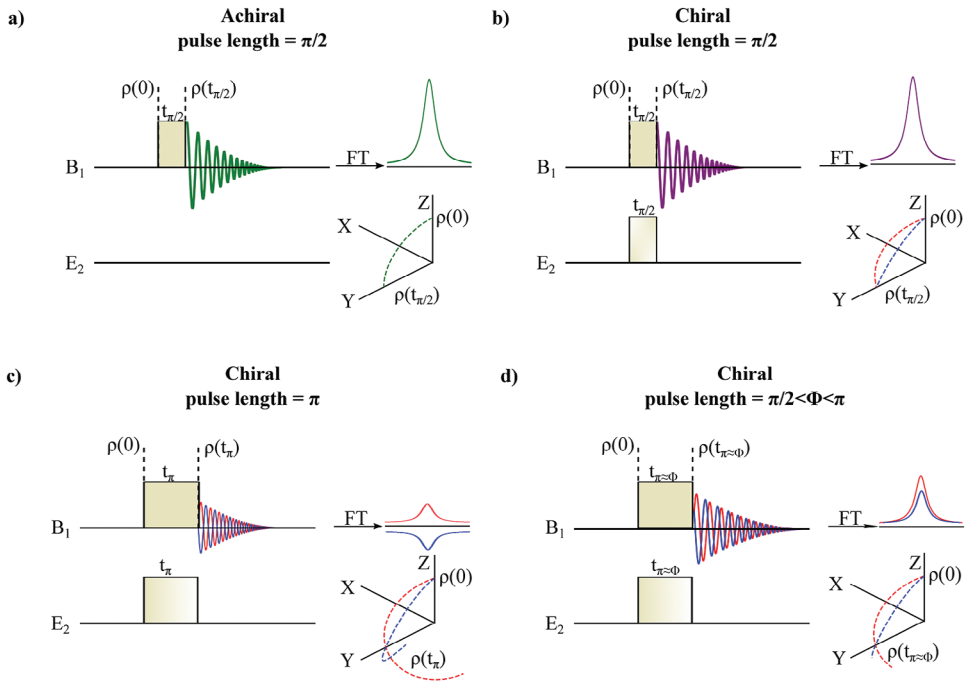

Figure 1. Summary of the evolution of magnetization for different pulse conditions, where blue and red curves show the magnetization trajectory of the two enantiomers. a) The case for a conventional NMR measurement, when only a magnetic pulse is applied. The signal for a chiral molecule will be similar to the acquisition from an achiral molecule. (b–d) In the presence of an electric field, a difference in the magnetization's trajectory is produced. However, depending on the angle by which the magnetization is flipped different situations will arise. b) When the net magnetization is flipped by $\pi/2$, the final chiral signal will be indistinguishable and hence similar to (a). c) The ideal case for a chiral measurement, when the net magnetization is flipped by an angle of π radians. In this case, the free induction decay (FID) recorded by the coil for the enantiomer pairs will be similar in magnitude but opposite in phase. d) The situation when the magnetization is flipped in the range $\phi \in (\pi/2, \pi)$. The FID recorded for two enantiomers will have the same phase but a difference in magnitude.

been the placement of a coil, tuned to the Larmor frequency, and matched to 50Ω, between the capacitor plates creating the electric field. However, this could disturb the chirally-sensitive volume of the exciter resonator, and adversely affect the device's detectivity. A solution proposed was to shuttle the liquid between the exciter and the detector. This could be challenging, given the space restrictions in a superconducting NMR magnet's bore, since the exciter and detector would need to be placed apart with enough distance, such that the sensitive volume is not disturbed. In addition, the sample's placement in the resonator and the sample's dielectric properties would have disturbed the chirally sensitive volume. No attempt at an implementation has yet to be successful.

Therefore, there remains a need for a detector design which could both excite the chiral component of the NMR signal sufficiently to render it detectable, and simultaneously suppress any signal due to the Zeeman part of the Hamiltonian. In this work, we present a novel microstrip-based detector which technically fulfills the requirements, and together with a suitable pulse sequence, demonstrates a measurement of the chiral signal. The resonator revealed an emerging oscillating magnetic moment when an RF electric field pulse $E_2(t)$ was applied to a chiral molecular sample. The article elaborates on the methodology and the physics behind the chiral signal, and **Figure 1** provides an overview of the article.

2. Results and Discussion

2.1. Spin Dynamics

In NMR, when a sample is placed in a magnetic field B_0, the spins (which act like small magnetic dipoles) align along the direction of B_0. Depending on the arrangement of the molecules, the aligned spins precess about the magnetic field direction with different frequencies. When an RF pulse is applied, some of the spins are tipped towards the plane normal to the B_0. After the application of the RF pulse, the spins relax to their initial phase during which they precess about the B_0 direction, which is the free-induction decay (FID). The precession of the spins produces the magnetic signal. This magnetic signal is acquired by a detector close to the sample, which reveals the NMR spectrum with a range of frequency shifts after Fourier transformation, as shown in Figure 1a. However, regardless of a molecule's handedness, the signal obtained for either enantiomer will be identical in structure. Therefore, an important aspect of measuring a chiral signal is to excite a chirality-dependent odd parity tensor in the Hamiltonian.[16] However, due to the lower magnitude of the tensor, compared to the Zeeman magnetization, one needs to suppress the signal obtained from the normally precessing magnetic dipole. To find a way to do this we followed the approach from Walls et al.[17], in which the time-independent NMR Hamiltonian

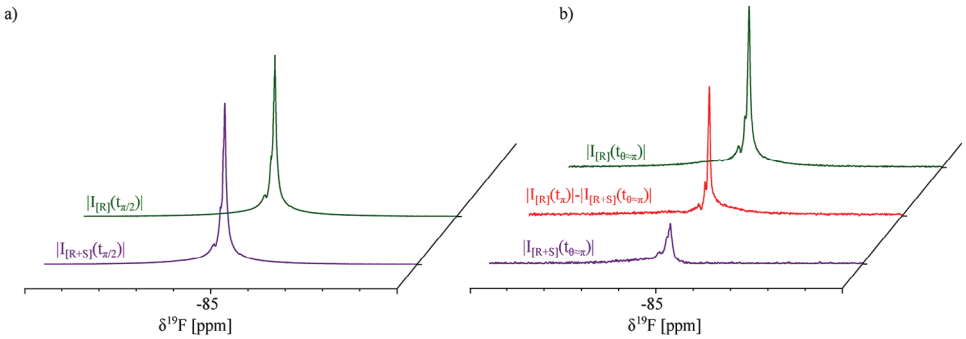

Figure 2. a) Comparison of the spectrum obtained for a racemic, and that of an enantiopure sample, both acquired after a $\pi/2$ pulse. The intensity magnitude for both samples was equal. The spectra were obtained with identical pulse parameters. There is no discernable difference. b) Intensity magnitudes under additional action of an RF electric field pulse, together with an equally long π magnetic pulse. The net effect together with the stray magnetic field produced by RF electric field and the magnetic field produced by the B_1 port flipped the net magnetization $\approx\pi$, where the (middle, red) curve is the computed difference between the racemic (R+S, lower purple curve) and the enantiopure sample's spectrum (R, green curve). The non-zero difference between the spectra confirmed the sign inversion effected by the electric field on each enantiomeric NMR signal.

for a nucleus at a chiral center in the presence of an applied RF electric field can be written as

$$\hat{H}_{\text{chiral}} = \Omega\hat{I}_z - \omega_{B_1}\hat{I}_x \mp \omega_{E_2}\hat{I}_y \tag{1}$$

where $\Omega = \omega_0 - \omega_{\text{rf}}$, with $\omega_0 = \gamma B_0$. Here, ω_{B_1} is the usual NMR RF excitation applied to the B_1-port of the resonator, and $\omega_{E_2} = \sigma_c E_2 \gamma B_0$ is the newly introduced electric field excitation term to induce the chiral signal and applied to the E_2-port of the two-port resonator as shown in Figure 5a. The chirality tensor σ_c possesses an opposite sign for each of the two enantiomers of a chiral center. After applying an electric and magnetic RF perturbation, the NMR Hamiltonian transforms to

$$\hat{\rho}(t_\theta) = \hat{I}_z \cos\omega_{E_2} t_\theta \cos\omega_{B_1} t_\theta \mp \hat{I}_x \sin\omega_{E_2} t_\theta \cos\omega_{B_1} t_\theta + \hat{I}_y \sin\omega_{B_1} t_\theta \tag{2}$$

where θ is the angle by which the net magnetization is flipped w.r.t to the B_0 direction and t_θ is the RF pulse duration required to reach this angle. Three scenarios can occur depending on the RF pulse applied to the electric field capacitor. If we apply an RF pulse for a time $t_{\pi/2}$ and as B_1 tip angle and E_2 tip angle are different,

$$\omega_{B1} t_{\pi/2} = \pi/2 \tag{3}$$

$$\omega_{E2} t_{\pi/2} \neq \pi/2 \tag{4}$$

such that the net magnetization is flipped by $\pi/2\text{rad} \equiv 90°$ as suggested in Buckingham and Fischer,[16] the density of states after time $t_{\pi/2}$ would be

$$\rho(t_{\pi/2}) = \hat{I}_y \tag{5}$$

In this case, the chiral term vanishes and the NMR signal from the enantiomers will be indistinguishable, see Figure 1b. The NMR signal acquired for [R], [S], or a racemic mixture will be equivalent to an achiral signal. If instead, we apply an RF excitation pulse for double the time, $t_\pi = 2t_{\pi/2}$ where,

$$\omega_{B1} t_\pi = \pi \tag{6}$$

$$\omega_{E2} t_\pi \neq \pi \tag{7}$$

such that the magnetization is flipped by $\pi\text{rad} \equiv 180°$, the density of states would reach

$$\rho(t_\pi) = -\hat{I}_z \cos(\omega_{E_2} t_\pi) \pm \hat{I}_x \sin(\omega_{E_2} t_\pi) \tag{8}$$

As can be gathered from the solution of the equation, the chiral term no longer vanishes during spin evolution, hence the NMR signal of the R and S enantiomers will have an opposite phase, Figure 1c, which cancels out in a racemic mixture. If, however, the net magnetization is flipped to an angle ϕ such that $\phi \approx \pi\text{rad}$ where only,

$$\omega_{B1} t_\phi \approx \pi \tag{9}$$

the signal intensity, Figure 1d, will be given as

$$\hat{\rho}(t_\theta) = \hat{I}_z \cos\omega_{E_2} t_\phi \cos\omega_{B_1} t_\phi \mp \hat{I}_x \sin\omega_{E_2} t_\phi \cos\omega_{B_1} t_\phi + \hat{I}_y \sin\omega_{B_1} t_\phi \tag{10}$$

Since the detector is sensitive to the magnetic moment along the x-y-plane, only the transverse projection of the density-of-states $\rho(t)$ will be measurable, leading to a peak intensity difference. A complete derivation of the signal due to both enantiomers is provided in the Supporting Information.

2.2. Proof of Principle

Since these were the first ever measurements to be recorded we started with the ^{19}F-spectroscopy of 1,1,1-trifluoropropan-2-ol, as this molecule was suggested to have the strongest chiral signal[18,19] in conjugation with ^{19}F. It contains three ^{19}F nuclei, which have a high gyromagnetic ratio and are the molecule's heaviest nuclei. If we had not observed the chiral effect with this molecule, it was an indication that we had a mistake in the proposed theory or the design of the detector. Therefore, a simple test to check the chiral effect was to observe the intensity variation when the net magnetization is aligned close to π. For this,

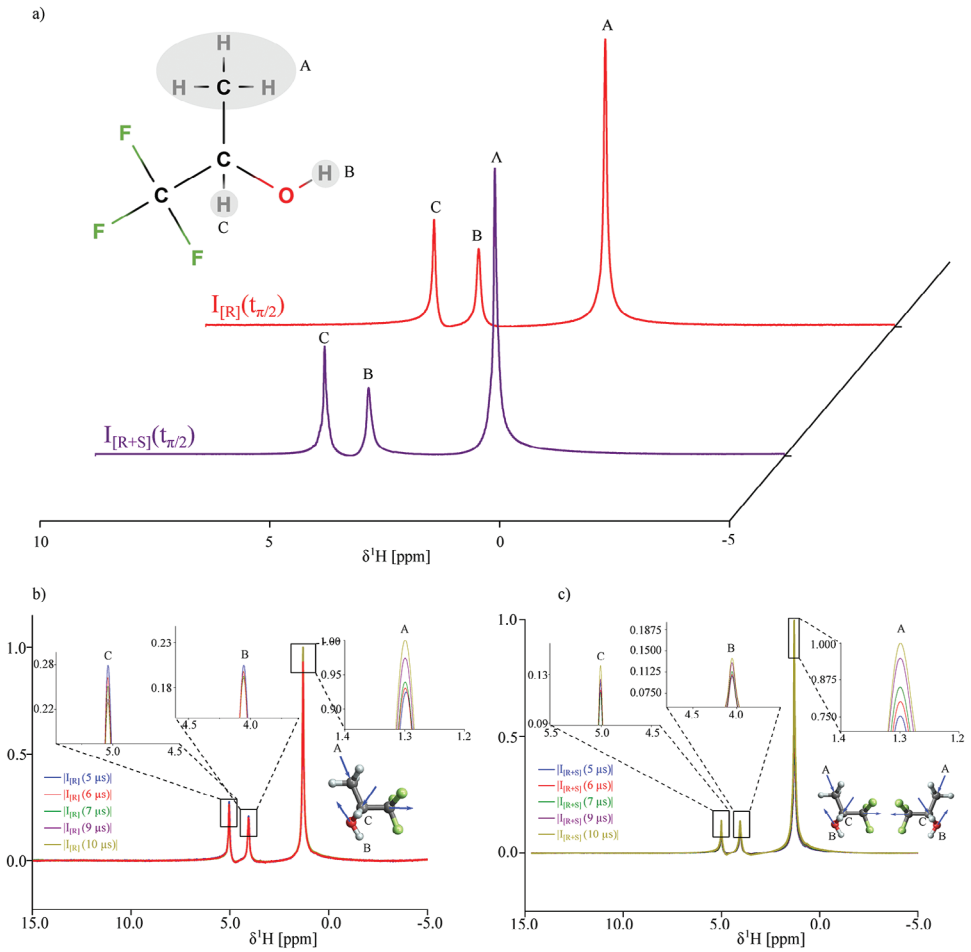

Figure 3. a) ^{1}H NMR spectrum acquired for 1,1,1-trifluoropropan-2-ol at a $\pi/2$ pulse length for the racemic and an R-enantiomeric sample. The capital letter labeling a peak represents the signal from the corresponding ^{1}H as labeled in the chemical structure. The chemical structure shown is a 2D representation, with the blue arrows in (b) and (c) indicating the direction of the electric dipoles, and are not scaled to the actual values. b) ^{1}H NMR spectrum acquired for 1,1,1-trifluoropropan-2-ol close to a π pulse length for the (R)-enantiomeric sample. The letter labeling the peaks in the inserts represents the signal from the ^{1}H labeled in the chemical structure shown in (a). The intensity of the peak labeled **A** increases with increasing pulse length of E_2, and the intensity of peaks labeled **B** and **C** reduce with increasing pulse length. c) The same experiment was repeated on the racemic sample. In this case, the intensity of the peaks labeled **A**, **B**, and **C** increase with increasing pulse length of E_2.

a comparison between a racemic and either of the enantiomers was enough. We compared the ^{19}F signal intensity from the $-CF_3$ group of the (R)-enantiomer with that of the racemic sample. The signal acquired for these samples using a $\pi/2$ pulse length, in the presence of an RF electric field, is shown in **Figure** 2a. The chiral signal acquired using pulse length that flipped the net magnetization approximately by π is shown in Figure 2b. The chiral signal was approximately 8% of the intensity at $\pi/2$, which is close to the prediction by,[18] where they estimated the value to be in the range of 1%–5% of an achiral signal. From the measurement results the chirality tensor for the ^{19}F atoms in 1,1,1-trifluoropropan-2-ol, was calculated to be 1.4×10^{-10}mV^{-1}. For more detail about the calculation please refer to the Supporting Information of this paper.

Next, identical measurements were repeated for the same molecule using ^{1}H spectroscopy. The relative intensity of the two peaks B and C, compared to peak A, was different for the racemic and (R)-enantiomer in $\pi/2$ pulse length acquisitions. Therefore, different pulse lengths for the electric field were used to investigate the behavior of each peak. The results obtained are plotted in **Figure** 3. The magnitude of the chirality tensor for the ^{1}H was compared to that of ^{19}F, and their ratio was found to be similar to the range predicted by[16]; however, we measured stronger magnitudes as compared to their predictions by simulation. The chirality constants at the 1.30, 4.05, and 5.00ppm peaks were found to be 6.0×10^{-11}, 4.8×10^{-11}, and 4.8×10^{-11}mV^{-1} respectively.

The complete set of measurement results and the calculations are presented in the Supporting Information. We also observed an even stronger chiral effect than predicted. Furthermore, we were unable to procure the other isomer, hence we decided to continue the measurements with the easily available enantiomer and its racemate, as discussed further.

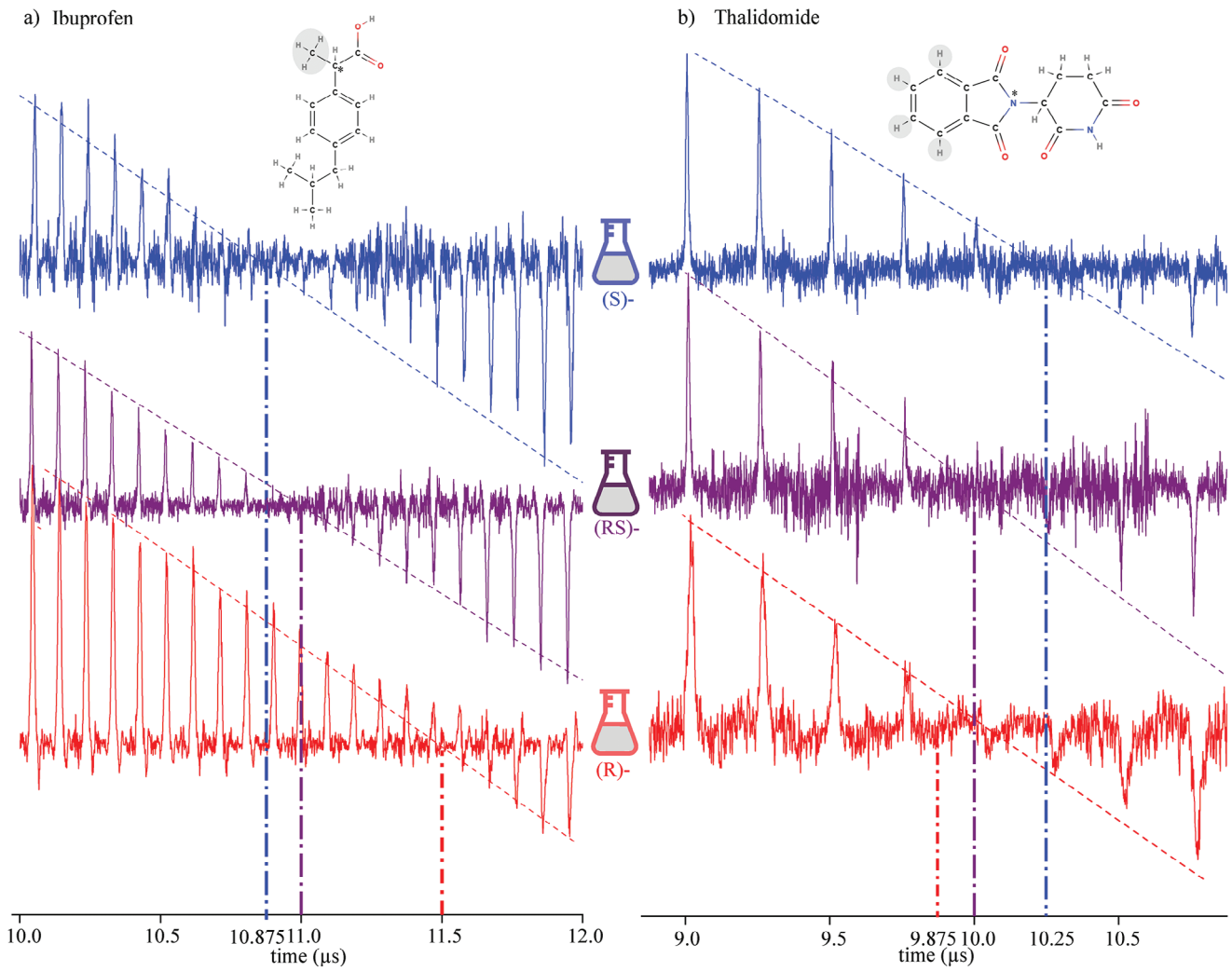

Figure 4. The figure shows excerpts of nutation spectra recorded for the ibuprofen (0.500 M in $CDCl_3$) and thalidomide (0.113 M in $DMSO - d_6$) samples, for the proton positions that are shaded in grey in the chemical structure diagrams. Blue represents (S)-enantiomer, purple represents racemate, and red represents (R)-enantiomer. The protons selected were those closest to the chiral center and hence possessed the largest chirality-dependent deviations of their spin dynamics. The power and the pulse length on the E_2 channel was kept constant at 20 W, for a duration of 10 μs. The power on the B_1 port was kept at a level of 20 W, and the pulse lengths were varied. A chirality-dependent coupling of electric and magnetic dipoles was observed, with the time required to align the magnetization to π dependent on the molecule and chiral center. The associated coupling factor, though not always equal in magnitude, is opposite in sense for the enantiomer pairs. The dotted line represents the theoretical nutation curve, plotted using Equation (10), with the coupling constant values taken from our measurement results, to determine the zero crossing point of the nutation line.

2.3. Enantiomer Distinction of Ibuprofen and Thalidomide

Since the chirality constant was measured to be stronger than originally expected, we decided to investigate the detection sensitivity with two further compounds, ibuprofen (0.500 M in $CDCl_3$), and thalidomide (0.113 M in DMSO-d_6). The reason for choosing a high concentration was that the chiral was reported to be sensitive to the spin density.[20] Therefore, with these concentrations, we could ensure that it did not affect normal NMR acquisitions, and the chiral effect could be observed. The minimum concentration up to which we observe the chiral effect still needs to be investigated. The apparatus used for the experiments, i.e., the sample, RF detector, and the ambient conditions, were such that the system remained under the RASER threshold.[21] Therefore, there could be no spontaneous emissions. Ibuprofen is used as a non-steroidal anti-inflammatory medication,[22] where only the (S)-enantiomer has therapeutic effects; however, the (R)-enantiomer undergoes chiral inversion during the metabolization process.[23] Thalidomide is infamous for the thalidomide scandal[3–5] and is a perfect example of the harmful effect of having the wrong enantiomer metabolized in a host's body.

To measure the chirality constant, we acquired nutation spectra for ibuprofen (**Figure** 4a) and thalidomide (Figure 4b) using three different enantiomer concentrations. These were the (R), the (S), and the racemic. The nutation spectra were recorded by varying the pulse lengths of the RF magnetic field, while the pulse length of the RF electric field was kept constant. The nutation experiments were performed on the peaks close to the chiral center,

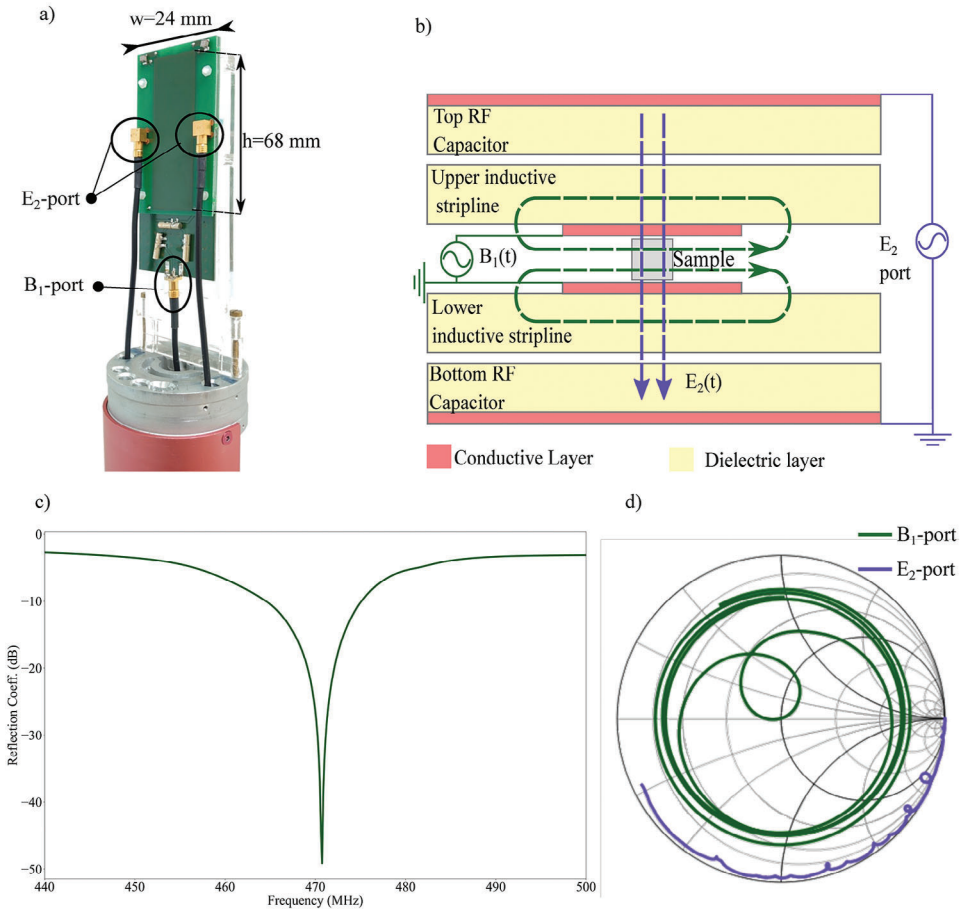

Figure 5. a) Chiral NMR detector, mounted on a commercial NMR probehead. b) Schematic of the chiral detector viewing toward the (positive) *z*-axis, where the B_0 field is pointing outside the paper, with two RF ports, and the four metal layers that bias the sample and detect its NMR response (figure not to scale). The sample is sealed in a square glass capillary with an inner side wall of 0.7mm. The sample is placed between the inductive inner layers of the detector. c) Measured reflection curve for the detector's magnetic port, for ^{19}F spectroscopy, after correct tuning and matching. The low reflection parameter value improves signal transmission and detection quality. d) Measured Smith chart for the two RF signals plotted for the range 440 to 500 MHz. The inner curve (green) shows the response of the Tx/Rx NMR port for the magnetic field signal, and the outer one (purple) the Tx port for the electric field signal.

and on those which experienced the strongest discerning effect, i.e., for ibuprofen and thalidomide, these were peaks at 1.48 and 8.00ppm, respectively.

From the measurement results, the chirality constants for the frequency shift at 1.48ppm for (R)- and (S)-ibuprofen were measured to be -1.65 × 10^{-10} and 4.89 × 10^{-11} m V^{-1}, respectively. The chirality constants for the frequency shift at 8.00ppm for (R)- and (S)-thalidomide were measured to be 4.60 × 10^{-11} and -9.20 × 10^{-11} m V^{-1}, respectively.

The difference in the chirality constant for thalidomide could be explained by the process of chiral inversion, or as reported by,[24] self-disproportionation of enantiomers. For thalidomide, it is now a well-documented process in which the (R)-enantiomer converts to the (S)-enantiomer.[25] This could be the reason why the chirality constant of (R) was measured to be lower than (S). Since the samples were stored in sealed glass capillaries, the difference in the sign indicates that the (R)- counterpart still had an enantiomeric excess (e.e.), and that the conversion process was not as fast in vitro as observed in vivo.

The ibuprofen, which was dissolved in $CDCl_3$ and stored in the sealed capillaries, also revealed a chemical or structural change. As can be seen from Figure S2 (Supporting Information), the signal from the carboxyl group started to appear after a certain time. As reported by the supplier of the chemical,[26] the signal from the carboxyl group should be silent. This peak was present in the (R)-enantiomer and the racemic of ibuprofen. We could not ascertain whether the (S)-enantiomer underwent chiral inversion over time, so that a structural change of (S) could not be ruled out, as ibuprofen could have several structural conformers,[27] of which a certain conformer is preferred in $CDCl_3$ solutions.[28] This may have led to variations in the chiral constant magnitudes. The detailed measurement results and calculations are presented and further elucidated in the Supporting Information.

3. Experimental Section

Normally, by applying an inversion RF magnetic pulse π to a spin-polarized sample, the resulting magnetization would be aligned

opposite to the direction of B_0, and hence would show no free induction decay signal during relaxation. Two conditions must be met before an observable signal can arise from an inverted magnetization. First of all, the sample must contain a sufficient excess of chiral molecules of a particular enantiomer, each excess molecule being equipped with an induced electric dipole of a particular sign at its selected chiral center. Second, a separate electric field RF pulse must be applied to the sample, simultaneously with the magnetic field pulse. However, applying an RF electric field comes with its challenges, as it produces an RF-associated magnetic field, which itself will influence the magnetic dipoles. For the detector used in the investigation, if only an electric field was applied, the stray magnetic field produced was measured to be ≈5.1 kHz for ^{1}H (or 120 μ T) with 20 W of power applied to the *E*-field port. This produced an electric field magnitude of 54k V m^{-1}. However, there would be a condition at which the effect of the magnetic field would be minimized after a finite pulse duration, as can be calculated from the Equation (10). The time required would be fairly long and in the range of ≈100 μs. Therefore, an excellent RF homogeneity have to be ensured in order not to lose signal intensity due to loss of spin coherence over time. If only a DC electric field had been used, a chiral effect might not had been observed.[17] All of these issues did not arise if a combined E_2-field and B_1-field π excitation were used. With the application of the electric field, and compensating the stray magnetic field, the reciprocity principle between electric and magnetic dipoles would then ensure their coupling, thus imposing a small deflection torque onto the downward-pointing magnetization. This deflection would result in a small detectable NMR signal in the free induction decay, proportional to the strength of coupling (or σ_c) between the electric and magnetic dipole of the enantiomer.

The accumulated phase of the chiral signal depended on the handedness of the molecule, which among two enantiomers, was due to the sign-inversion of the electric dipole. For the case that a nonchiral sample was subjected to a simultaneous radio-frequency magnetic and electric field pulse, no NMR signal would arise, due to the absent coupling between the electric and magnetic dipoles. Furthermore, a 50–50 racemic mixture produced no NMR signal since the free induction decays of the two enantiomers would be out of phase by exactly $\phi = \pi$, and hence cancel each other. Only an excess of one of the two enantiomers in a non-racemic sample produced an observable signal.

From the above discussion, the requirements of the detector could now be derived. Since the odd parity term, which distinguishes the spin dynamics of the enantiomers, was proportional to the magnitude of the impinging electric field, the detector should be able to apply strong electric field excitations to the sample. As the chiral signal became stronger when the magnetic dipoles were flipped by angles of multiples of π, the detector should be able to apply highly uniform magnetic field excitations to avoid dephasing of the magnetization. The detector should also have the ability to control the electric and magnetic fields individually, under full spectrometer control.

The detector in precision printed circuit board technology as a stack of four striplines which symmetrically sandwich the sample, **Figure** 5a,b was implemented. The inner layers corresponding to the B_1-port were formed by the inductively-tuned striplines that create a strong time-dependent magnetic field $B_1(t) \perp B_0$ perpendicular to the axis of the striplines, and parallel to their planes, whilst minimizing any stray electric field. The outer capacitively-tuned stripline planes corresponding to the E_2-port were made relatively wide, to reduce their stray magnetic field component, and due to the proximity of the two faces to the sample, produced a strong time-dependent electric field $E_2(t) \perp B_0$, hence transverse to both the B_0 axis and the stripline planes. As a result, $B_1(t) \perp E_2(t)$. The sample was confined to a thin capillary placed along the longitudinal symmetry axis of the stack, along the B_0 axis. Within its sample volume, the electric and magnetic fields remained strictly perpendicular to each other. The striplines were electrically tuned to retain their RF properties across a wide band of frequencies (Figure 5c,d).

The measurements were performed on an 11.74 T vertical wide-bore superconducting NMR spectrometer (Bruker AVANCE III) with the bespoke detector (this work) mounted on a customized probe head (Voxalytic GmbH), as shown in Figure 5a. The samples were prepared identically, ensuring that the sample volumes were the same (2.94 μl). The sample volume was limited in depth by the distance of the capacitor plates used for the E_2 fields. Since the magnitude of E_2 varies inversely with the distance between the capacitor plates, it is advantageous to keep them as close as possible. However, the minimum distance was limited by the size of the capillary that could be used, where the size of the capillary was limited by the process of filling and sealing it. For the measurements, the capillaries used were a square capillary (from CM Scientific Ryefield (EU) Ltd., Ireland) with outer side wall of 0.98mm and inner side wall of 0.7mm. The length of the sample was limited by the homogeneous region of the B_1 field of the detector which was 6mm. Therefore, this resulted in the given volume. The shimming values for different experiments were within an acceptable range of each other, such that no deviation was observed in the NMR lineshape.

4. Conclusion

In this paper, we demonstrated a method to directly distinguish chiral enntiomers using NMR spectroscopy. The principle of the method was based on the evolution of magnetization for a chiral molecule in an NMR environment under the action of a simultaneously applied external RF electric field. It was shown that, depending on the angle by which the net magnetization is flipped from its initial position, the chiral signal was distinguishable for $\theta \neq \pi/2$. Based on this, a detector was designed which was capable of producing B_1 and E_2 RF fields orthogonal to each other. Three molecule sets were tested, 1,1,1-trifluoropropan-2-ol, ibuprofen, and thalidomide, to demonstrate the theory established, and the correct functioning of the detector. To further investigate the effect on naturally occurring chiral molecules, alanine with the molar concentration of 0.830 M in D_2O was investigated as it is one of the stable chiral molecules. The measurement results are reported in the Supporting Information. Since it is a newly developed method developed, there is still a wide range of chiral molecules that need to be further investigated and to develop pulse sequences to elucidate enantiomeric differences rather than pure enantiomeric samples.

As the concentration may affect the chiral signal,[20] therefore, the chances to observe the effect may reduce for molecules that cannot be dissolved at such high concentration. At this moment,

we did not investigate the effect of concentrations on the measurements; however, one solution may be to increase the number of acquisitions or to develop a long-duration electric field pulse sequence, which accumulates the chiral signal analogous to the increasing number of acquisitions.

The detector was designed for chiral elucidation measurements in NMR. However, it could also be used for chiral-induced spin selectivity (CISS) experiments. In ref. [29] the authors discovered differences in the enantiomer signal intensities using cross-polarization, and concluded that the reason could be due to the physics behind CISS. We believe that, with full control of RF electric and magnetic fields, it should be possible to investigate these and other effects, which have remained elusive to date.

Supporting Information

Supporting Information is available from the Wiley Online Library or from the author.

Acknowledgements

J.G.K. acknowledges Prof. Dr. Peer Fischer for discussions on the topic of enantiomer-selective NMR, and Prof. Dr. Ulrike Wallrabe for checking the manuscript. S.W. acknowledges Dr. Ronald Kampmann for help in sample preparation, and Dr. Dario Mager for providing strong support for the project during SW's time as a PhD candidate at KIT. J.G.K. and S.W. acknowledge discussions with Dr. Neil MacKinnon, Dr. Mazin Jouda, Prof. Dr. Stefan Bräse, and Prof. Dr. Burkhard Luy. The authors also thank the staff at **Voxalytic GmbH**, Germany for the quick adaptation of their NMR probehead according to our requirements. The authors acknowledge the Helmholtz Research Area Information, in its program Materials Systems Engineering, for a **VirtMat** scholarship for S.W., the **ERC SygG 951459 HiSCORE**, for supporting D.B. and J.G.K., and the **CRC 1527 HyPERiON** funded by the DFG for supporting JGK.

Open access funding enabled and organized by Projekt DEAL.

Conflict of Interest

J.K, is a shareholder in Voxalytic GmbH, a company that sells NMR equipment.

Author Contributions

The concept was initialized by J.G.K., for which he acquired the funding. S.W. and J.G.K. formulated the theory, and realized the detector design. The NMR experiments were performed by S.W., and verified by J.G.K.. D.B. prepared thalidomide and alanine samples, and helped clarify the chemical concepts. S.W. wrote the initial manuscript draft. All authors contributed equally to iterate the manuscript.

Data Availability Statement

The data that support the findings of this study are available from the corresponding author upon reasonable request.

Keywords

chirality, drug discovery, enantiomeric excess, NMR

Received: June 16, 2024
Revised: August 2, 2024
Published online:

[1] J. Mc.Conathy, M. J. Owens, *The Prim. Care Companion J. Clin. Psychiatry* **2003**, *5*, 70.
[2] L. A. Nguyen, H. He, C. Pham-Huy, *Int. J. Biomed. sci.: IJBS* **2006**, *2*, 85.
[3] G. Blaschke, H. P. Kraft, K. Fickentscher, F. Kohler, *Arzneim.-Forsch.* **1979**, *29*, 1640.
[4] M. Landoni, A. Soraci, *Curr. Drug Metab.* **2001**, *2*, 37.
[5] M. G. Nilos, J. Gan, D. Schlenk, *Effects of Chirality on Toxicity*, John Wiley & Sons, Ltd, Hoboken, New Jersey **2009**.
[6] M. Raban, K. Mislow, *Tetrahedron Lett.* **1965**, *6*, 4249.
[7] G. Whitesides, J. Lewis, *J. Am. Chem. Soc.* **1970**, *92*, 6979.
[8] D. Parker, *Chem. Rev.* **1991**, *91*, 1441.
[9] I. Canet, J. Courtieu, A. Loewenstein, A. Mddour, J. Pechine, *J. Am. Chem. Soc.* **1995**, *117*, 6520.
[10] R. Schwenninger, J. Schlögl, J. Maynollo, K. Gruber, P. Ochsenbein, H.-B. Bürgi, R. Konrat, B. Kräutler, *Chem. - Eur. J.* **2001**, *7*, 2676.
[11] C. M. Thiele, *Eur. J. Org. Chem.* **2008**, *2008*, 5673.
[12] H. Duddeck, E. D. Gómez, *Chirality* **2009**, *21*, 51.
[13] G. Kummerlöwe, B. Luy, *Trends Anal. Chem.* **2009**, *28*, 483.
[14] T. J. Wenzel, C. D. Chisholm, *Chirality* **2011**, *23*, 190.
[15] A. D. Buckingham, *Chem. Phys. Lett.* **2004**, *398*, 1.
[16] A. D. Buckingham, P. Fischer, *Chem. Phys.* **2006**, *324*, 111.
[17] J. D. Walls, R. A. Harris, *J. Chem. Phys.* **2014**, *140*, 234201.
[18] P. Garbacz, P. Fischer, S. Krämer, *J. Chem. Phys.* **2016**, *145*, 104201.
[19] P. Garbacz, J. Cukras, M. Jaszuński, *Phys. Chem. Chem. Phys.* **2015**, *17*, 22642.
[20] P. Garbacz, *Mol. Phys.* **2018**, *116*, 1397.
[21] S. Lehmkuhl, S. Fleischer, L. Lohmann, M. S. Rosen, E. Y. Chekmenev, A. Adams, T. Theis, S. Appelt, *Sci. Adv.* **2022**, *8*, eabp8483.
[22] World Health Organization, World Health Organization model list of essential medicines: 22nd list (2021), Technical documents, **2021**.
[23] S. C. Tan, B. K. Patel, S. H. D. Jackson, C. G. Swift, A. J. Hutt, *Br. J. Clin. Pharmacol.* **2003**, *55*, 579.
[24] J. Han, O. Kitagawa, A. Wzorek, K. D. Klika, V. A. Soloshonok, *Chem. Sci.* **2018**, *9*, 1718.
[25] E. Tokunaga, T. Yamamoto, E. Ito, N. Shibata, *Sci. Rep.* **2018**, *8*, 17131.
[26] Sigma–Aldrich, FT-NMR Spectra, https://www.sigmaaldrich.com/deepweb/assets/sigmaaldrich/quality/spectra/287/458/FNMR008613.pdf (accessed: March 2024).
[27] M. Vueba, M. Pina, L. B. de Carvalho, *J. Pharm. Sci.* **2008**, *97*, 845.
[28] I. Khodov, S. Efimov, V. Klochkov, G. Alper, L. B. de Carvalho, *Eur. J. Pharm. Sci.* **2014**, *65*, 65.
[29] J. I. Santos, I. Rivilla, F. P. Cossío, J. M. Matxain, M. Grzelczak, S. K. S. Mazinani, J. M. Ugalde, V. Mujica, *ACS Nano* **2018**, *12*, 11426.